

We are IntechOpen, the world's leading publisher of Open Access books Built by scientists, for scientists

6,200

Open access books available

169,000

International authors and editors

185M

Downloads

Our authors are among the

154

Countries delivered to

TOP 1%

most cited scientists

12.2%

Contributors from top 500 universities



WEB OF SCIENCE™

Selection of our books indexed in the Book Citation Index
in Web of Science™ Core Collection (BKCI)

Interested in publishing with us?
Contact book.department@intechopen.com

Numbers displayed above are based on latest data collected.
For more information visit www.intechopen.com



Nanomaterials of Carbon and Metal Sulfides in Photocatalysis

Ana C. Estrada, Joana L. Lopes and Tito Trindade

Abstract

Heterogeneous semiconductor photocatalysis has received much interest because of its applications in important global energy and environmental challenges in a cost-effective sustainable way. The photocatalytic efficiency of semiconductor photocatalysts under solar irradiation has been pointed out by difficulties associated with low visible-light absorption range, fast recombination of photogenerated carriers, and low chemical stability in operational conditions. Graphitic materials have attracted great interest due to properties, such as high surface area, mechanical strength, and photochemical stability. Thus, their combination with metal sulfides, has been explored as promising strategies to produce new photocatalysts. These nanocomposites show great potential in photodegradation of contaminants of emerging concern (CEC), which might be detected in water sources, such as traces of Pharmaceuticals and pesticides. Here, we briefly review fundamental principles photocatalysis in general, with the focus on the use of carbon-nanomaterials of distinct structural dimensionalities associated with nano-crystalline metal sulfides, envisaging their application as heterogeneous photocatalysts for water remediation. Key aspects concerning the photocatalyst properties, such as light absorption, charge separation and transfer, and stability, are also approached. Graphene and graphene derivatives have demonstrated great potential for increasing photogenerated charge-carrier separation and migration efficiency, as well as in extending the light absorption range and adsorption capacity.

Keywords: metal sulfide, carbon nanomaterials, photocatalysis, water treatment

1. Introduction

Photocatalyst is a term that combines two words—*photo*, which is related to light, and *catalyst*, which is a compound that does not change the thermodynamics of the reaction but changes its kinetics, by establishing new reaction routes with lower activation energy, without being consumed during the process. Hence, semiconductor photocatalysis involves chemical reactions that occur at the surfaces of certain semiconductor compounds when irradiated with light of a selected wavelength range. Typically, these reactions occur in a liquid medium using the photocatalyst in the solid state, thus the chemical process is generally termed heterogeneous photocatalysis. In

this work, the semiconductor photocatalyst is considered as part of a colloid or suspension, though this has not been always the case. For instance, thin films have been also applied namely for air purification. Examples of heterogeneous photocatalytic processes using semiconductor particles include photooxidation reactions, which have been exploited for the degradation of organic pollutants present in water [1–5]. Compared to more conventional water treatment methods, such as those based on adsorption and flocculation, which might require a subsequent step for the chemical degradation of the pollutant, in photocatalysis the pollutant is eliminated by aerobic photooxidation. Ideally, this oxidative process should generate carbon dioxide and water as the final products, that is, the complete mineralization of the organic pollutant, though this has been rarely achieved. As such, different remediation technologies can coexist in the same water treatment plant and, in several situations, their complementary role brings more efficient approaches. For example, adsorption and photocatalytic technologies can be implemented in different stages in the same water treatment plant. Even though, advanced oxidation processes based on the use of efficient photocatalysts have been regarded as a way to minimize the impact of CEC in water sources, which even in trace levels are harmful and for which conventional water treatments are ineffective.

Two main optical processes have been proposed considering the role of the semiconductor during a photocatalytic reaction, as illustrated in **Figure 1** for TiO₂ photocatalysts. In direct photocatalysis, a photon with energy higher than the band gap energy of the semiconductor ($h\nu_1$) is absorbed and an electron (e^-) is excited to the conduction band (CB), leaving a hole (h^+) in the valence band (VB). The band gap energy of the semiconductor is defined as the difference between the CB (bottom energy level) and the VB (top energy level). The photogenerated electron–hole pair ($e^-/–h^+$) is responsible for reduction and oxidation reactions that take place at the surface of the photocatalyst particle in contact with the aqueous medium. The electron in the CB migrates to the surface of the semiconductor and participates in reduction reactions, and the hole in the VB diffuses to the photocatalyst surface and is involved in oxidation reactions. In addition, the dissolved O₂ can accept photogenerated electrons to yield superoxide radicals ($O_2^{\bullet-}$) and photogenerated holes can oxidize H₂O to form strong oxidant hydroxyl radicals (HO^\bullet) (Eqs. (1) and (2)) [6, 7].

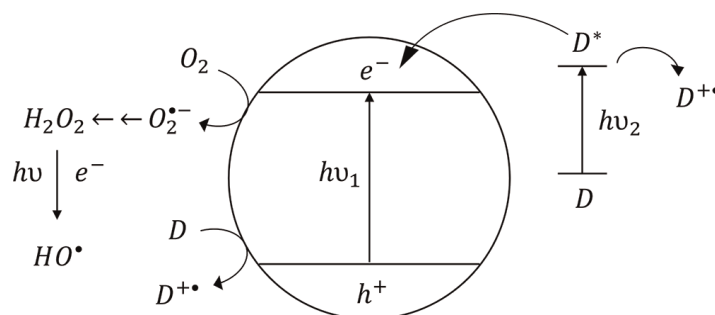
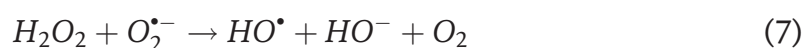
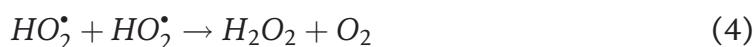


Figure 1. The schematic representation of the direct ($h\nu_1$) and indirect ($h\nu_2$) photochemical processes occurring in light-irradiated TiO₂ nanoparticles, commonly used as photocatalysts in the form of aqueous colloids. Adapted from [6].

On the other hand, in indirect photocatalysis, also known as photosensitized photocatalysis, the mechanism involves the photoexcitation ($h\nu_2$) of a second species (P) to an excited state from which an electron is injected into the CB of the semiconductor. This process has been observed in the degradation of contaminant organic dyes, which can also act as photosensitizers for cases in which the reduction potential of the excited state is negative enough for electron injection into the CB of the semiconductor [7]. In indirect photocatalysis, there is no generation of a VB hole and the semiconductor functions as an electron relay, thereby preventing undesired back reactions [7]. Nevertheless, this process is usually less efficient than direct photocatalysis due to the lower efficiency of the electron injection. Both direct and indirect photocatalysis convert the initially generated superoxide radicals into other reactive oxygen species with high oxidative power (Eqs. (3)-(7)), for example, with reduction potentials of 0.94 V ($O_2^{\bullet-}/H_2O_2$), 1.29 V (H_2O_2/H_2O) and 1.90 V (HO^{\bullet}/HO^-) [6, 8]. Although such radicals are nonselective, they are effective in oxidizing organic contaminants, such as dye molecules [9–15], antibiotics [16–20], or pesticides [21–25], as well as for other sanitation applications, such as the elimination of pathogens [26–32].



In semiconductor photocatalysis, several fundamental aspects should be considered to develop the photocatalyst based on functional and operational criteria. Hence, light absorption (absorption coefficient and wavelength range), photoinduced charge separation, charge trapping, and charge transfer are among the key parameters for designing efficient photocatalytic systems [33, 34]. For instance, photogenerated electrons are unstable species in an excited state, which tend naturally to return to the ground state either via adsorbed hydroxyl radicals or by recombination with unreacted holes or structural traps on semiconductors [35–38]. Since these species are determinants in the efficiency of a photocatalyst, several research groups have explored strategies to increase the photoinduced charge separation to avoid charge recombination and consequently increase the lifetime of photogenerated electron/hole pairs. These strategies include (i) coupling of semiconductor photocatalysts with metal nanoparticles [39–41]; (ii) sensitization of the photocatalyst surface through physical or chemical adsorption of molecules that absorb visible light and are excited either to the singlet or triplet excited state [42] and; (iii) coupling of at least two semiconductor photocatalysts with different bandgap values [43, 44]. The presence of charge trapping sites in a semiconductor photocatalyst allows also the extension of the lifetime of the charge carriers from microseconds to milliseconds since in these sites there is greater charge-carrier stability. Although such trap sites are mostly located at the surface of a semiconductor photocatalyst, they may be present also on grain boundaries or in the bulk lattice, or even present as electron scavengers, such as O_2 . On the other hand, deeply stabilized trapped charges lose redox potential and increase the potential barrier for charge transfer at the semiconductor or water interface [45].

Thus, electron transfer reaction depends largely on structural parameters ascribed to the semiconductor photocatalyst, such as crystal facet structure, lattice surface, size, and morphology. Trapping mechanisms might be favorable if they allow photon activity to generate charge carriers, and permit charge carriers to reach the electron transfer regions. Otherwise, it could be disadvantageous for the overall photocatalytic process.

Several strategies have been proposed to adjust the physical and chemical properties of semiconductor photocatalysts to improve light absorption and charge transfer efficiency, reduce the recombination rate of photogenerated charge carriers, and accelerate surface reactions [46]. Examples of such strategies include metal-ion doping of the semiconductor [39–41], combination with distinct semiconductors that result in heterostructures [43, 44], and surface chemical functionalization using selected photosensitizers [42]. Noteworthy, the combination of inorganic semiconductors with carbonaceous materials, such as graphene and their structural derivatives, has also received great attention in the design of a new class of nanocomposite photocatalysts [47, 48]. The use of carbon nanostructures for supported semiconductor photocatalysts offers great advantages. Hence, depending on the carbon material, high electrically conductive nanostructures can act as scavengers of photogenerated electrons. Also, water-compatible nanomaterials promote the aqueous dispersion of the photocatalyst, which by achieving a high specific surface area enhances the adsorption capacity of the system [48]. Furthermore, surface functionalization of the carbon lattice confers functional chemical groups that might favor the subsequent attachment of semiconductor nanophases. A paradigmatic example of this situation is the application of graphene oxide as a nanopatform for semiconductor photocatalysts, and notwithstanding limitations that can also arise such as photoreduction of the carbon substrate or the limited absorption by the photocatalyst [49–51].

2. Metal-sulfide photocatalysts

In general terms, a good photocatalyst should have the following characteristics: effective charge-carrier separation, fast charge transfer, strong optical absorption, photochemical stability, low-cost production, and nontoxicity [52]. Among the several types of photocatalysts available, inorganic semiconductors have been intensely investigated in water remediation processes because they might fulfill, at least in selected cases, the above requirements. Inorganic materials considered as semiconductors exhibit bandgap energies in the range of 0.3–3.8 eV. In particular, TiO₂ and TiO₂-based heterogeneous photocatalysts have been the most explored semiconductor materials for photocatalytic applications because of the high free energy of photogenerated charge carriers, low-cost, and high chemical stability [53, 54]. However, both TiO₂ polymorphs (anatase/rutile) show a wide bandgap (anatase 3.2 eV; rutile 3.0 eV), which limits photocatalytic applications of pure TiO₂ to UV irradiated systems. Other semiconductor photocatalysts exhibiting narrower bandgaps have been investigated, which can replace TiO₂ in certain conditions or that might act as a complementary phase in extending light absorption to the visible composite systems. Among these semiconductors, this chapter focus on the use of binary metal-sulfide compounds, with emphasis on their nanocrystalline forms. **Table 1** shows examples of metal sulfides investigated as photocatalysts and selected properties for the pure phases.

Metal sulfide	Bandgap energy (eV)*	Structure
ZnS	3.6	Cubic, Hexagonal
CdS	2.4	Cubic; Hexagonal
CuS	2.4	Hexagonal
Ag ₂ S	1.0	Monoclinic
Bi ₂ S ₃	1.4	Orthorhombic

Table 1.
 Characteristics of macrocrystalline metal sulfides as photocatalysts in an aqueous medium [44].

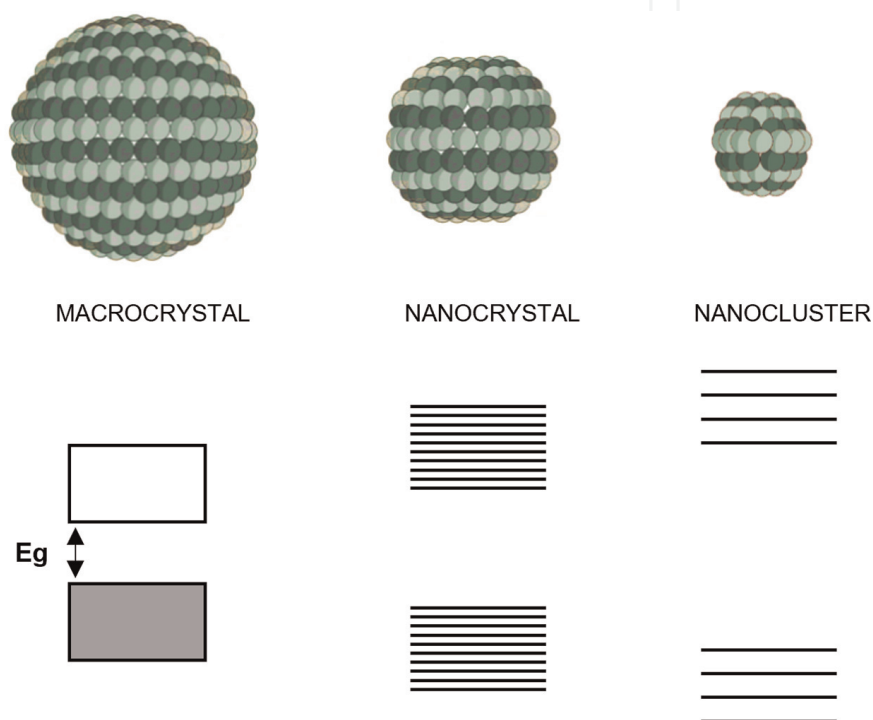


Figure 2.
 The scheme illustrates the widening of the bandgap energy of a certain semiconductor material, as particle size decreases from its macrocrystalline form (left) to the nanocluster regime (right). Quantum dots are nanocrystalline semiconductors (middle) that show quantum-size effects, corresponding to the intermediate situation between macrocrystalline materials and nanoclusters.

A macrocrystalline metal sulfide (MS) semiconductor comprises a three-dimensional network of ordered atoms (metal and S atoms) characterized by a band gap energy at a certain temperature. As particle size decreases, and below a certain threshold, the electronic band structure of the semiconductor changes with the widening of the bandgap energy [55, 56]. For semiconductor nanoclusters, that is molecular-like nanocrystals depicted on the right in **Figure 2**, an analogous interpretation applies, although the energy gap is usually understood as the energy separation between the frontier molecular orbitals HOMO (highest occupied molecular orbital) and LUMO (lowest unoccupied molecular orbital). Thus, as in the case of conventional photoconductors, the incidence of a photon with energy greater than this energetic separation originates in semiconductor nanocrystals (and nanoclusters) the formation of an electron-hole pair, often called exciton, which in the macrocrystalline material is dimensionally characterized by the Bohr exciton radius of that

semiconductor. The charge carriers in nanosized semiconductors migrate fast and participate in several photoprocesses, which include trapping and recombination [57, 58].

Metal sulfides can be explored in the macrocrystalline form as photocatalysts, for example, in aqueous suspensions, membranes, and thin films [59–61]. However, in the past decades, there has been intense research on their use as nanocrystalline materials, namely due to the possibility to explore quantum-size effects, as mentioned above. MS semiconductor nanocrystals (quantum dots) are small crystalline particles that exhibit quantum size-dependent optical and electronic properties [62, 63]. With typical dimensions in the range of 1–100 nm, these nanocrystals bridge the gap between those of molecules and micrometric crystals, displaying distinct optical behavior in relation to their bulk counterparts [64]. If the size of nanocrystals is smaller than the bulk exciton Bohr radius, the charge carriers become spatially confined, showing size-dependent absorption and fluorescence spectra with discrete electronic transitions at room temperature (**Figure 2**).

For instance, the optical spectra of colloids of nanocrystalline semiconductors show blue shifts in their absorption edges (or excitonic peaks) with decreasing particle diameters. Metal-sulfide nanocrystals that exhibit quantum size effects, that is, quantum dots, can be used as size-tuned light-absorption photosensitizers, namely in visible photocatalytic applications [44, 65–67]. Quantum size effects occurring in MS nanocrystals dispersed in aqueous suspensions, also affect the CB and VB redox levels, thus influencing redox reactions that involve the migration of photogenerated charge carriers to the particles' surfaces. Nanosized semiconductors have dimensions considerably superior to conventional molecular photosensitizers, which in comparison to the latter, present a broader absorption wavelength range, large density of states, and high optical extinction coefficients [62], hence favoring photon harvesting in photocatalytic applications.

Colloidal synthesis offers a wide range of chemical methods to obtain MS nanocrystals with controlled particle size distributions and particle shapes, thus with tailored bandgaps for diverse semiconductors and their solid solutions [68–71]. Furthermore, such colloids can be selected as nanodispersed systems showing strong visible-light absorption and size-tuned bandgap. However, these systems also show limitations, which deserve further research aiming their application as more efficient photocatalysts. Although certain MS is used as visible-light photocatalysts, the photogenerated electron-hole pairs are also susceptible to recombination. The occurrence of charge-carrier recombination limits their mobility from the bulk lattice to the particles' surface, thus decreasing the efficiency of the photocatalyst. Moreover, surface-sulfide anions (S^{2-}) in aqueous MS colloids are prone to oxidation, a process that gains more relevance due to the oxidative role of photogenerated holes at the surface [72, 73]. In fact, under light irradiation, sulfide anions can oxidize forming sulfate (SO_4^{2-}) or elemental sulfur (S^0), causing the deactivation of the photocatalyst.

The inhibition of metal-sulfide photocorrosion is an important requirement for photocatalytic reactions, namely because the long lifetime of photogenerated electron-hole pairs and the chemical stability are essential for producing efficient photocatalysts. Several strategies have been reported that tackle this problem, such as modifying the crystal structure, size, and morphology of semiconductors [74, 75], combining with transition metal ions or cocatalysts [76, 77], producing heterojunctions, [78–80] and by adjusting the reaction parameters [81–83]. For instance, Bo *et al.* have reported that the interfacial interaction between both semiconductors in the MoS_2/CdS heterostructures restrains the photocorrosion of MoS_2 .

The authors have shown that electrons photogenerated on the CB of CdS are transferred to the CB of MoS₂ to participate in the H₂ evolution reaction, while the holes on the VB of MoS₂ migrate to the VB of CdS [79]. Huang *et al.* have shown that the growth of a larger bandgap semiconductor, such as ZnO, on a core with a smaller band gap as CdS improves the stability of the hybrid nanostructure and inhibits the photocorrosion of CdS particles [84]. In turn, Yi and Wang have found that the photocorrosion of CdS is significantly inhibited when cobalt ions or molybdate are injected into the CdS-lactic acid system. The photogenerated holes in the CdS are fastly captured by the transition metal ions, reducing the oxidation of S²⁻ on the CdS surface [85, 86]. The coupling of metal-sulfide semiconductor photocatalysts with inorganic substrates might bring other advantages and several approaches have been reported [87, 88]. In this context, carbon nanomaterials have also been investigated as functional platforms that bring new potential to the application of these materials, including photocorrosion inhibition of the supported metal sulfides.

3. Carbon-based nanostructures

The development of heterogeneous photocatalysts by combining metal sulfides and different carbon nanomaterials has been explored as an effective strategy to obtain high-performance photocatalysts. Owing to delocalized electrons from the conjugative π -system, graphitic carbon nanostructures are good at accepting and shuttling the photogenerated electrons from semiconductor photocatalysts; hence, effectively separating the electron-hole pairs [89–93]. For instance, Wan *et al.* have shown that the synergistic influence of charge-carrier migration, advanced excited states, and suitable Fermi levels between CdS phases and graphene leads to enhanced photoactivity and stability [94]. Also, Lv *et al.* have shown that graphene attached to semiconductors can efficiently accommodate and transport electrons from the excited semiconductor, which not only hindered charge recombination but also improved charge transfer, giving rise to high photocatalytic efficiency [89]. These works confirmed the relevant role of graphene, among the carbon-based nanomaterials, in aqueous colloidal chemistry processes, such as heterogeneous photocatalysis. Thus, in this chapter, graphene and its derived nanostructures are used as illustrative examples in the fabrication of carbon-supported metal-sulfides photocatalysts.

Graphene is a 2D material formed by a one-atom-thick planar layer of sp²-hybridized carbon atoms that resemble a chicken-wire-shaped lattice, presenting outstanding electronic, thermal, and mechanical properties [95]. Graphene is the basic structural material of graphite, which result from the overstacking of graphene monolayers *via* van der Waals forces, resulting in interspaced neighboring layers that are 0.34 nm far apart [96, 97]. The carbon atoms in each graphene sheet establish covalent bonds due to the overlapping of trigonal planar sp² hybrid orbitals. The overlapping of the perpendicular unhybridized p_z orbitals accounts for the formation of the VB and the CB, respectively composed of filled π orbitals and empty π^* orbitals [98].

The mechanical exfoliation of graphite creates free-standing graphene sheets, as shown by Novoselov and Geim, who used sequential micromechanical cleavage of graphite using the “scotch-tape method.” The authors were honored with the Nobel Prize in Physics in 2004, 6 years later to such an important finding [98, 99]. The direct exfoliation of bulk graphite produces layers of graphene with good quality and crystallinity, low defect densities, and high conductivity, but frequently, at a low yield

[100]. As such, graphene layers can be obtained by the chemical exfoliation of a low-cost raw material bulk graphite, which applied together with selected chemicals produce graphene and graphene derivatives, such as GO and reduced graphene oxide (rGO) [100–102]. Although water is a first-choice medium for the production of graphene-based materials, the hydrophobic nature of pristine graphene sheets tends to promote their restacking, which makes exfoliation challenging. The use of surfactants during the exfoliation processes has been considered to overcome this limitation because they allow exfoliated layers to remain suspended and avoid overstacking [101, 103]. The success of the exfoliation processes is overcoming the van der Waals forces by increasing the distance between the layers *via* chemical intercalation. Ideally, to obtain good dispersion of graphene layers, the solvents should have surface tensions of 40 mJ/m² [97, 101, 104]. Therefore, graphene can be exfoliated by the sonication of graphite in dimethylformamide (DMF), N-methyl-2-pyrrolidone (NMP), pyridine, and perfluorinated compounds [98, 101, 104, 105]. For instance, Hernandez *et al.* have used sonication-based exfoliation of graphite in NMP to obtain a final material containing graphene monolayers (28%) and nanosheets less than six atomic layers thick, almost in quantitative yield [106]. Commonly used sonication exfoliation processes involve shear forces and cavitation mechanisms, which involve the growth and collapse of micrometer-sized bubbles, acting on the bulk material precursor and causing their exfoliation [97].

GO is composed of sp² graphene layers with a high content of oxygen-containing functional groups, such as hydroxyl, epoxy, carboxylic, and carbonyl groups [107]. The UV–visible absorption spectra of GO suspensions show an absorption peak ascribed to π - π^* electronic transitions of aromatic C-C bonds and n- π^* transitions of the oxygen-containing groups, at around 230 nm and 315 nm, respectively [108]. The aqueous suspensions of GO are normally stable due to the hydrophilic character of oxygen-containing groups present in the sheets' surfaces, namely at the edges. Colloidal stability is favored by the electrostatic repulsion that arises due to anionic groups that form due to extensive proton dissociation in such functional groups, over a certain pH range. On the other hand, the presence of out-of-planar C-O covalent bonds increases the interlayer distance from 0.34 to 0.65 nm, therefore decreasing the energy needed to separate the graphene layers [96, 98, 107]. The hydrophilic nature of oxidized graphite facilitates water to be adsorbed into its lamellar structure, showing a further increase in the interlayer distance to 1.15 nm [109]. For instance, the use of polar solvents (e.g., ethanol, acetonitrile, and dimethyl sulfoxide) allows the preparation of stable colloids but either flocculation or aggregation occur when nonpolar organic solvents are used as the dispersing medium [107].

Carbon nanotubes (CNT) are 1D materials formed by graphene sheets rolled around a common axis, with diameters reaching between 0.5 and 100 nm, and lengths extending several micrometers or even millimeters [110]. CNT can be single- (SWCNT) or multi-walled (MWCNT) according to the number of graphene sheets rolled-up, that is, a single sheet or more than one, respectively. SWCNTs have diameters in the range of 1–2 nm and MWCNT show typical diameters in the range of 10–100 nm range [111]. Pristine CNT has hydrophobic nature, and their high aspect ratio favors interparticle van de Waals forces mediated by the outer walls, which results in a tendency for CNT aggregation [112]. Thus, non-functionalized CNT dispersed in a liquid medium exists as large bundles, which limit handling and, consequently, their use in many applications. Usually, mechanical disentanglement of CNT bundles is achieved by ultrasonication of the respective dispersions in which shear forces promote the separation of CNT but can also cut such nanostructures.

Nevertheless, the debundling process depends on the modification of the CNT surface by using chemical agents that enhance the compatibility of the CNT with the dispersing medium. Hence, surface modifiers, such as surfactants, homopolymers, and block copolymers, have been used to promote the dispersion of CNT in aqueous environments. In addition, surface oxidation treatments that result in the presence of carboxylic, hydroxyl, and carbonyl functional groups at the end of the tubes and on their sidewalls, also allow better dispersions of CNT in water [113].

Powder X-ray diffraction (XRD) has been used to check the crystalline structure of graphitic materials. Bulk graphite shows a strong Bragg diffraction peak at 26.6° corresponding to the reflection of (002) planes and associated with an interlayer distance of 0.34 nm. The oxidation and exfoliation of graphite increase the interlayer distance changing the peak position of the basal (002) reflection from 26.6 to 11.2° , which corresponds to an interplanar distance of 0.79 nm, as observed for GO materials [98].

Raman spectroscopy has been a key instrumental technique to study graphene materials, such as the surface chemistry of GO and the existence of structural defects. The Raman spectra of graphitic materials are typically characterized by three distinct vibrational bands: the G-, D-, and 2D-bands. The G-band is observed around 1580 cm^{-1} and is ascribed to the in-plane bending mode of the sp^2 hybridized carbon atoms in graphene. In high-quality graphene, this band is very sharp, suggesting its high crystallinity and non-defect structure. The D-band at around 1350 cm^{-1} has been associated with the amount and type of defects in the carbon lattice, for example, the existence of sp^3 hybridization or due to vacancies [114]. The extension of such defects in the carbon sheet, either at the edges or topological defects, have been monitored by Raman measurements using such diagnosis band, namely by computing the intensity ratio between the G- and D-bands [98, 104, 114]. In the Raman spectrum of high-quality pristine graphene, the D-band is not observed or is very weak, but it is observed in GO samples due to the presence of different oxygen functional groups in the carbon sheets. Hence, the D-to-G Raman band intensity ratio provides useful information on the nature and extension of structural defects that characterize the GO samples [94]. The 2D band is an overtone of the D-band, resulting from a two-photon lattice vibrational process. For true single-layer graphene, such a band occurs as a symmetric feature below 2700 cm^{-1} [104, 114]. Overstacking of successive layers results in structures of less symmetry with a Raman shift to higher wavenumbers [98]. For example, in graphite and graphite oxide materials, it is observed a broad band at about 2800 cm^{-1} . The features of the G and 2D bands are particularly useful in exfoliation and surface modification laboratorial tasks because are the first indication for distinguishing between monolayer (or few-layer) graphene and graphite-based materials. Furthermore, it has been shown that Raman methods applied to GO modified with metal sulfides are an alternative strategy to probe the surface of nanocomposite photocatalysts [115].

4. Application of carbon-based semiconductor nanostructures in photocatalysis

Metal sulfides, such as the binary compounds CdS, Ag₂S, Bi₂S₃, and CuS, have been referenced in photocatalysis literature as efficient photon harvesters of visible-light radiation [116]. When supported on graphitic materials, these semiconductors improve the conductivity for electron capture and transport [51, 117–123]. There are

several methods of synthesis of metal sulfides coupled to rGO and GO substrates, which comprise solid-state, sonochemical, microwave irradiation, solvothermal, and hydrothermal methods [113, 120, 121, 124–138]. Our research group has developed a single-source method to prepare GO-based composites having supported metal sulfides. The type of metal sulfide generated *in situ* is determined by the metal dialkyldithiocarbamate complex employed as a single-molecule precursor, thus GO-based nanocomposites of Ag₂S, CuS, Bi₂S₃, and ZnS, are examples of such materials (**Figure 3**) [131]. In fact, this method is an extension of the sonochemical method first developed by Estrada *et al.* for decorating MWCNT, GO, and graphite with CdS obtained from the precursor cadmium(II) diethyldithiocarbamate [113].

Although CdS presents serious drawbacks for practical applications due to its well-known toxicity, research on CdS-based nanomaterials provide helpful insights concerning the visible-light response and underlying mechanisms in semiconductor photocatalysis [139]. There are a number of studies reporting visible-light active heterostructures of CdS/rGO and CdS/GO, which were investigated as photocatalysts for the degradation of organic dyes [124, 126, 128]. These heterostructures showed higher photocatalytic efficiency than bare CdS and could be used for up to four cycles, without loss of activity. For instance, Zhang *et al.* developed visible-light irradiated CdS/graphene nanophotocatalysts for the photooxidation of alcohols and reduction of Cr(VI) ions in water [140]. Multicomponent photocatalysts of TiO₂/CdS/rGO have shown higher photocatalytic activity than TiO₂/rGO, for the photodegradation of RhB, MB, and *p*-chlorophenol, under visible-light irradiation [141, 142]. Wang *et al.* showed that nanocomposites based on heterojunctions of CdS and TiO₂ nanoparticles were efficiently supported on rGO [141]. Such heterostructures prevented CdS photocorrosion due to the synergy that results from supporting such coupled semiconductor nanostructures on rGO (**Figure 4**). Similarly, the coupling of semiconducting phases, such as TiO₂ and CdS or Ag₂S, improves photon harvesting and charge separation and prevents the oxidation of the metal sulfides [142, 143].

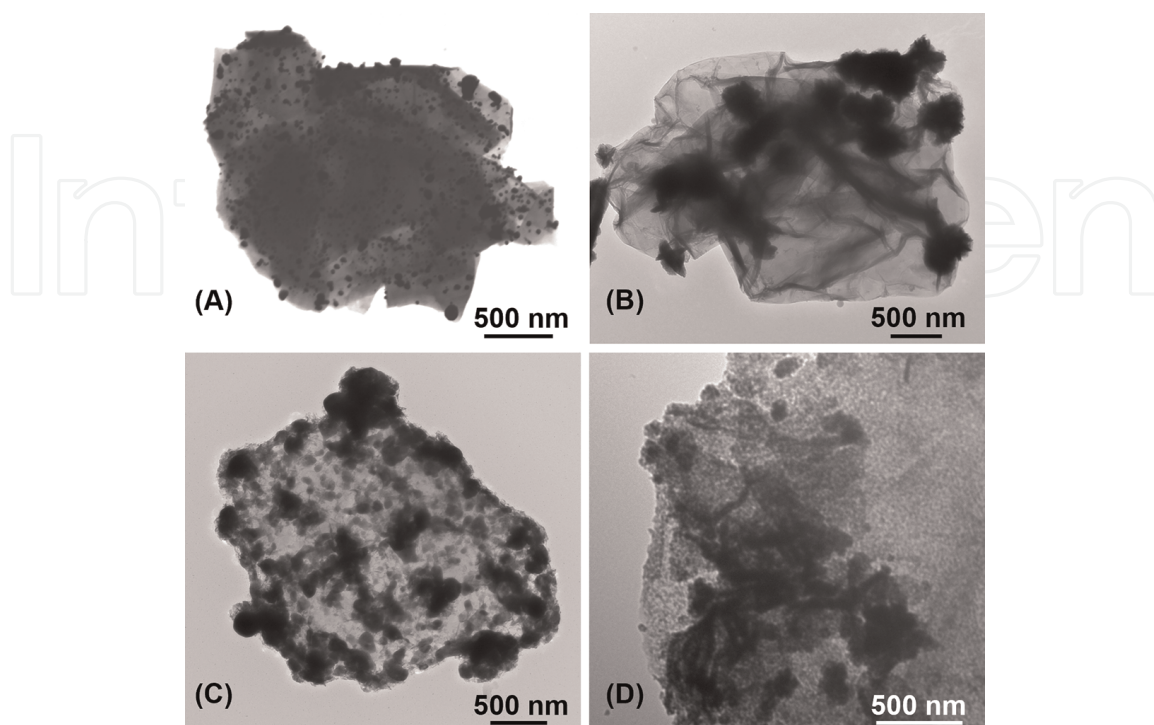


Figure 3. TEM images of heterostructures of graphene oxide decorated with (A) Ag₂S, (B) CuS, (C) Bi₂S₃, and (D) ZnS.

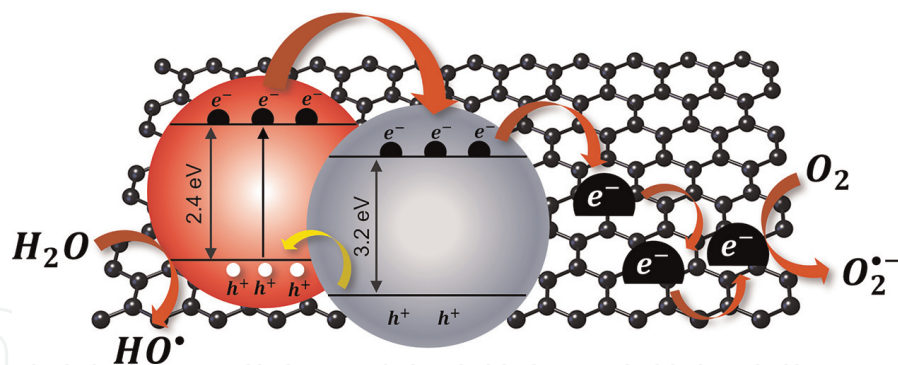


Figure 4. The scheme illustrates visible-light photogeneration of oxygen radicals in a hybrid heterostructure composed of CdS (red)/TiO₂ (gray) supported on rGO sheets dispersed in an aqueous medium.

The semiconductor Bi₂S₃ absorbs in the visible and NIR spectral range and does not pose serious toxicity concerns associated with CdS. Wang and coworkers showed that Bi₂S₃ immobilized on carbon dots have higher photocatalytic efficiency than their individual components, by investigating the degradation of MB and tetracycline under UV-, visible-, and NIR-light irradiation [144]. Khalid *et al.* synthesized nanorods of Bi₂S₃, which showed 87% efficiency in the degradation of Congo red dye, under UV-light irradiation over 90 minutes [145]. Chen *et al.* have reported improved photodegradation of 2,4-dichlorophenol irradiated with visible light in the presence of Bi₂S₃/rGO nanocomposites [137]. The authors also found that there is an optimal loading of Bi₂S₃ phases on carbon substrates, concluding that for higher contents of rGO less efficient photocatalytic systems are obtained. Similarly, for Ag₂S/graphene, it was found that the performance of the photocatalyst depended on the relative amounts of semiconductor and graphene in the nanostructure. The authors have investigated samples with distinct graphene content (wt%: 2, 4, and 6), showing that in those conditions, the photodegradation of RhB, occurred most efficiently under visible-light irradiation in the presence of the sample 4 wt% in graphene [146].

Copper sulfide is a *p*-type semiconductor with phase-dependent properties; thus, the band gap energy range between 1.2 and 2.2 eV, depending on the crystalline form present [147–151]. This is an interesting aspect for photocatalytic applications because several crystalline phases have been reported for copper sulfide, showing the metal in distinct oxidation states, such as in chalcocite (Cu₂S) and covellite (CuS). Additionally, several nonstoichiometric phases (Cu_{2-x}S) have been reported showing compositions that can be easily varied depending on the experimental conditions [152]. Hybrid nanostructures composed of copper sulfide and graphene (or graphene derivatives) show high potential in photocatalysis. For instance, it has been reported that hybrid nanostructures of CuS/rGO show superior photocatalytic activity as compared to the single-phase system composed of CuS nanoparticles, for the photodegradation of organic dyes under visible-light irradiation [121, 153–155] and UV-light irradiation [156]. El-Hout *et al.* have reported that CuS/rGO photocatalysts lead to the complete mineralization of malachite green after 90 minutes, under sunlight irradiation [157]. As previously mentioned, Shi *et al.* also stated that there is an optimal loading of CuS on rGO, showing that samples with 20% of rGO have better photocatalytic activity than samples containing 30% of rGO [120]. This has been explained by the effect on the stacking of graphene sheets and metal-sulfide particle aggregation, which results from the presence of a high amount of carbon nanomaterials (rGO or graphene) employed in the composite structure [155, 158]. Wang *et al.* have found that the

synergistic interaction occurring between graphene and metal-sulfide phases in CuS/graphene, with an impact on the electronic conductivity of graphene and CuS/graphene morphology, accounts for the observed stability and photoactivity of such heterostructures [159]. Matos *et al.* have synthesized hybrid composites comprising S-doped graphene decorated with CuS and Fe₃O₄ semiconductor phases, which showed higher photocatalytic ability than their individual components in the photodegradation of 4-nitrophenol, in addition, these photocatalysts could be recovered and reused in subsequent cycles [158].

Although ZnS is a non-absorbing material in the visible range due to its wide band gap energy (3.66 eV for blende structure and 3.77 eV for wurtzite structure), it has been found that ZnS coupled to carbon nanomaterials result in hybrid heterostructures with photocatalytic activity under visible-light irradiation [127, 133, 135]. Hence, Ming *et al.* have reported the degradation of ciprofloxacin, MB, and RhB under visible-light irradiation in the presence of ZnS/carbon nanostructures [160]. Also, Chen and Chakraborty have shown that under UV-light irradiation, the photodegradation of RhB and MO occurs more efficiently in the presence of the ZnS/graphene and ZnS/rGO photocatalysts, respectively [136, 161].

5. Conclusions

This chapter provided a concise overview on the use of graphene and graphene derivatives coupled to nanocrystalline semiconductors of metal sulfides in heterogeneous photocatalysis. For these applications, pure metal-sulfide nanoparticles show some limitations, which depending on the semiconductor include limited harvesting of photons in the visible region, low photocatalytic quantum yield, fast recombination of photogenerated charge carriers, and photocorrosion. Hence, several chemical strategies have been reported to improve photoefficiency and performance of these nanoparticles as photocatalysts. Metal-sulfide phases coupled with graphitic materials have been employed to prevent the photocorrosion of the chalcogenide semiconductor and to increase the photocatalytic efficiency of the resultant hybrid nanostructures. Particularly, graphene (and its derivatives) have shown great merits in improving the photogenerated charge-carriers separation and migration, also extending the light absorption range and the adsorption capacity of the photocatalysts. Furthermore, their use as supporting substrates in aqueous suspensions also inhibits the agglomeration of the particles, thus keeping exposed a high surface area to the photoactive semiconductors. The design of graphene-based materials decorated with metal sulfides as photocatalysts requires the assessment of the several parameters that might contribute to their performance in specific contexts. Hence, it has been reported that these hybrid nanostructures show optimal compositional features on the carbon nanomaterial and semiconductor, depending on the target pollutant and operational conditions. Furthermore, the surface functionalization of graphene materials also plays an important role in the development of such photocatalysts, namely the content load in the metal sulfide and their defect structure. Finally, the cost-effective production of graphene-based semiconductor nanocomposites at a large scale, envisaging their application as photostable and efficient heterogeneous photocatalysts, is still a great challenge. In the chemical design of such photocatalysts, eco-friendly up-scale strategies should be also addressed by researchers, to guarantee its future commercialization for environmental applications.

Acknowledgements


A.C. Estrada acknowledges the research position funded by national funds (OE), through FCT-Fundação para a Ciência e a Tecnologia, I.P., in the scope of the framework contract foreseen in the numbers 4, 5, and 6 of the article 23, of the Decree-Law 57/2016, of August 29, changed by Law 57/2017, of July 19. J. L. Lopes thanks FCT for the doctoral grant SFRH/BD/126241/2016. This work was developed within the scope of the project CICECO-Aveiro Institute of Materials, UIDB/50011/2020, UIDP/50011/2020 & LA/P/0006/2020, financed by national funds through the FCT/MEC (PIDDAC).

Author details

Ana C. Estrada*, Joana L. Lopes and Tito Trindade
CICECO-Aveiro Institute of Materials, Department of Chemistry, University of Aveiro, Aveiro, Portugal

*Address all correspondence to: ana.estrada@ua.pt

IntechOpen

© 2023 The Author(s). Licensee IntechOpen. This chapter is distributed under the terms of the Creative Commons Attribution License (<http://creativecommons.org/licenses/by/3.0>), which permits unrestricted use, distribution, and reproduction in any medium, provided the original work is properly cited. 

References

- [1] Yang X, Wang D. Photocatalysis: From fundamental principles to materials and applications. *ACS Applied Energy Materials*. 2018;**1**(12):6657-6693
- [2] Wang H, Li X, Zhao X, Li C, Song X, Zhang P, et al. A review on heterogeneous photocatalysis for environmental remediation: From semiconductors to modification strategies. *Chinese Journal of Catalysis*. 2022;**43**:178-214
- [3] Jabbar ZH, Esmail ES. Recent advances in nano-semiconductors photocatalysis for degrading organic contaminants and microbial disinfection in wastewater: A comprehensive review. *Environmental Nanotechnology, Monitoring & Management*. 2022;**17**:100666
- [4] Melchionna M, Fornasiero P. Updates on the roadmap for photocatalysis. *ACS Catalysis*. 2020;**10**:5493-5501
- [5] Dong S, Feng J, Fan M, Pi Y, Hu L, Han X, et al. Recent developments in heterogeneous photocatalytic water treatment using visible light-responsive photocatalysts: A review. *RSC Advances*. 2015;**5**:14610-14630
- [6] Kisch H. Semiconductor photocatalysis - Mechanistic and synthetic aspects. *Angewandte Chemie International Edition*. 2013;**52**:812-847
- [7] Pichat P, editor. *Photocatalysis and Water Purification: From Fundamentals to Recent Applications*. Weinheim, Germany: Wiley-VCH; 2013
- [8] Zeng X, Liu Y, Hu X, Zhang X. Photoredox catalysis over semiconductors for light-driven hydrogen peroxide production. *Green Chemistry*. 2021;**23**:1466-1494
- [9] Rafiq A, Ikram M, Ali S, Niaz F, Khan M, Khan Q, et al. Photocatalytic degradation of dyes using semiconductor photocatalysts to clean industrial water pollution. *Journal of Industrial and Engineering Chemistry*. 2021;**97**:111-128
- [10] Qutub N, Singh P, Sabir S, Sagadevan S, Oh WC. Enhanced photocatalytic degradation of Acid Blue dye using CdS/TiO₂ nanocomposite. *Scientific Reports*. 2022;**12**:5759
- [11] Saeed M, Muneer M, Haq AUL, Akram N. Photocatalysis: An effective tool for photodegradation of dyes - A review. *Environmental Science and Pollution Research*. 2022;**29**:293-311
- [12] Zhao Y, Li Y, Sun L. Recent advances in photocatalytic decomposition of water and pollutants for sustainable application. *Chemosphere*. 2021;**276**:130201
- [13] Rosu MC, Coros M, Pogacean F, Magerusan L, Socaci C, Turza A, et al. Azo dyes degradation using TiO₂-Pt/graphene oxide and TiO₂-Pt/reduced graphene oxide photocatalysts under UV and natural sunlight irradiation. *Solid State Sciences*. 2017;**70**:13-20
- [14] Bai L, Pan X, Guo R, Linghu X, Shu Y, Wu Y, et al. Sunlight-driven photocatalytic degradation of organic dyes in wastewater by chemically fabricated ZnO/Cs₄SiW₁₂O₄₀ nanoheterojunction. *Applied Surface Science*. 2022;**599**:153912
- [15] Yuan Y, Guo R, Hong L, Ji X, Li Z, Lin Z, et al. Recent advances and perspectives of MoS₂-based materials for photocatalytic dyes degradation: A review. *Colloid Surface A*. 2021;**611**:125836

- [16] Yang X, Chen Z, Zhao W, Liu C, Qian X, Zhang M, et al. Recent advances in photodegradation of antibiotic residues in water. *Chemical Engineering Journal*. 2021;**405**:126806
- [17] Wu S, Lin Y, Hu YH. Strategies of tuning catalysts for efficient photodegradation of antibiotics in water environments: A review. *Journal of Materials Chemistry A*. 2021;**9**:2592-2611
- [18] Roy N, Alex SA, Chandrasekaran N, Mukherjee A, Kannabiran K. A comprehensive update on antibiotics as an emerging water pollutant and their removal using nano-structured photocatalysts. *Journal of Environmental Chemical Engineering*. 2021;**9**:104796
- [19] Zhu XD, Wang YJ, Sun RJ, Zhou DM. Photocatalytic degradation of tetracycline in aqueous solution by nanosized TiO₂. *Chemosphere*. 2013;**92**: 925-932
- [20] Brice RP, Claire JC, Mouldi H, Vincent G, Carole CB, Gaël P. Photo-oxidation of three major pharmaceuticals in urban wastewater under artificial and solar irradiations. *Journal of Photochemistry and Photobiology A: Chemistry*. 2022;**425**:113673
- [21] Farner Budarz J, Cooper EM, Gardner C, Hodzic E, Ferguson PL, Gunsch CK, et al. Chlorpyrifos degradation via photoreactive TiO₂ nanoparticles: Assessing the impact of a multi-component degradation scenario. *Journal of Hazardous Materials*. 2019; **372**:61-68
- [22] Berberidou C, Kitsiou V, Kazala E, Lambropoulou DA, Kouras A, Kosma CI, et al. Study of the decomposition and detoxification of the herbicide bentazon by heterogeneous photocatalysis: Kinetics, intermediates and transformation pathways. *Applied Catalysis B: Environmental*. 2017;**200**: 150-163
- [23] Cruz M, Gomez C, Duran-Valle CJ, Pastrana-Martínez LM, Faria JL, Silva AMT, et al. Bare TiO₂ and graphene oxide TiO₂ photocatalysts on the degradation of selected pesticides and influence of the water matrix. *Applied Surface Science*. 2017;**416**: 1013-1021
- [24] Vaya D, Surolia PK. Semiconductor based photocatalytic degradation of pesticides: An overview. *Environmental Technology and Innovation*. 2020;**20**: 101128
- [25] El-Saeid MH, Baqais A, Alshabanat M. Study of the photocatalytic degradation of highly abundant pesticides in agricultural soils. *Molecules*. 2022;**27**:634
- [26] Regmi C, Joshi B, Ray SK, Gyawali G, Pandey RP. Understanding mechanism of photocatalytic microbial decontamination of environmental wastewater. *Frontiers in Chemistry*. 2018;**6**(33):1-6
- [27] Wu H, Inaba T, Wang ZM, Endo T. Photocatalytic TiO₂@CS-embedded cellulose nanofiber mixed matrix membrane. *Applied Catalysis B: Environmental*. 2020;**276**:119111
- [28] Hu X, Hu X, Tang C, Wen S, Wu X, Long J, et al. Mechanisms underlying degradation pathways of microcystin-LR with doped TiO₂ photocatalysis. *Chemical Engineering Journal*. 2017;**330**: 355-371
- [29] Soleimani M, Ghasemi JB, Mohammadi Ziarani G, Karimi-Maleh H, Badiie A. Photocatalytic degradation of organic pollutants, viral and bacterial pathogens using titania nanoparticles.

Inorg Chemistry Communication. 2021; **130**:108688

[30] Jalvo B, Faraldos M, Bahamonde A, Rosal R. Antimicrobial and antibiofilm efficacy of self-cleaning surfaces functionalized by TiO₂ photocatalytic nanoparticles against *Staphylococcus aureus* and *Pseudomonas putida*. *Journal of Hazardous Materials*. 2017; **340**:160-170

[31] Venieri D, Fraggadaki A, Kostadima M, Chatzisymeon E, Binas V, Zachopoulos A, et al. Solar light and metal-doped TiO₂ to eliminate water-transmitted bacterial pathogens: Photocatalyst characterization and disinfection performance. *Applied Catalysis B: Environmental*. 2014; **154-155**:93-101

[32] Aftab S, Shabir T, Shah A, Nisar J, Shah I, Muhammad H, et al. Highly Efficient Visible Light Active Doped ZnO Photocatalysts for the Treatment of Wastewater Contaminated with Dyes and Pathogens of Emerging Concern. *Nanomaterials*. 2022; **12**:486

[33] Zhou W, Fu H. Defect-mediated electron-hole separation in semiconductor photocatalysis. *Inorganic Chemistry Frontiers*. 2018; **5**:1240-1254

[34] Sah C-T, Shockley W. Electron-hole recombination statistics in semiconductors through flaws with many charge conditions. *Physics Review*. 1958; **109**(4):1103-1115

[35] Ahmed M, Dincer I. A review on photoelectrochemical hydrogen production systems: Challenges and future directions. *International Journal of Hydrogen Energy*. 2019; **44**(5): 2474-2507

[36] Acar C, Dincer I, Zamfirescu C. A review on selected heterogeneous

photocatalysts for hydrogen production. *International Journal of Energy Research*. 2014; **38**:1903-1920

[37] Bessegato GG, Guaraldo TT, de Brito JF, Brugnera MF, Zanoni MVB. Achievements and trends in photoelectrocatalysis: From environmental to energy applications. *Electrocatalysis*. 2015; **6**:415-441

[38] Garcia-Segura S, Brillas E. Applied photoelectrocatalysis on the degradation of organic pollutants in wastewaters. *Journal of Photochemistry and Photobiology C: Photochemistry Reviews*. 2017; **31**:1-35

[39] Devendran P, Selvakumar D, Ramadoss G, Sivaramakrishnan R, Alagesan T, Jayavel R, et al. A novel visible light active rare earth doped CdS nanoparticles decorated reduced graphene oxide sheets for the degradation of cationic dye from wastewater. *Chemosphere*. 2022; **287**: 132091

[40] Kočí K, Matějů K, Obalová L, Krejčíková S, Lacný Z, Plachá D, et al. Effect of silver doping on the TiO₂ for photocatalytic reduction of CO₂. *Applied Catalysis B: Environmental*. 2010; **96**: 239-244

[41] Choi W, Termin A, Hoffmann MR. The role of metal ion dopants in quantum-sized TiO₂: Correlation between photoreactivity and charge carrier recombination dynamics. *The Journal of Physical Chemistry*. 1984; **98**: 13669-13679

[42] Youssef Z, Colombeau L, Yesmurzayeva N, Baros F, Vanderesse R, Hamieh T, et al. Dye-sensitized nanoparticles for heterogeneous photocatalysis: Cases studies with TiO₂, ZnO, fullerene and graphene for water

purification. *Dyes and Pigments*. 2018; **159**:49-71

[43] Long R, English NJ, Prezhdov OV. Minimizing electron-hole recombination on TiO₂ sensitized with PbSe quantum dots: Time-domain Ab initio analysis. *Journal of Physical Chemistry Letters*. 2014; **5**:2941-2946

[44] Ayodhya D, Veerabhadram G. A review on recent advances in photodegradation of dyes using doped and heterojunction based semiconductor metal sulfide nanostructures for environmental protection. *Mater Today Energy*. 2018; **9**:83-113

[45] Mohamed HH, Bahnemann DW. The role of electron transfer in photocatalysis: Fact and fictions. *Applied Catalysis B: Environmental*. 2012; **128**: 91-104

[46] Zhang S, Ou X, Xiang Q, Carabineiro SAC, Fan J, Lv K. Research progress in metal sulfides for photocatalysis: From activity to stability. *Chemosphere*. 2022; **303**:135085

[47] Xiang Q, Yu J, Jaroniec M. Graphene-based semiconductor photocatalysts. *Chemical Society Reviews*. 2012; **41**:782-796

[48] Syed N, Huang J, Feng Y, Wang X, Cao L. Carbon-based nanomaterials via heterojunction serving as photocatalyst. *Frontiers in Chemistry*. 2019; **7**:1-7

[49] Thanh Doan Nguyen T, Nguyen D, Ngoc Doan H, Phong Vo P, Tan Huynh V, Ha Hoang V, et al. In-depth understanding of the photoreduction of graphene oxide to reduced-graphene oxide on TiO₂ surface: Statistical analysis of X-ray photoelectron and Raman spectroscopy data. *Applied Surface Science*. 2022; **581**:152325

[50] Spilarewicz-Stanek K, Jakimińska A, Kisielewska A, Dudek M, Piwoński I. Graphene oxide photochemical transformations induced by UV irradiation during photocatalytic processes. *Materials Science in Semiconductor Processing*. 2021; **123**: 105525

[51] Ahmad N, Sultana S, Sabir S, Khan MZ. Exploring the visible light driven photocatalysis by reduced graphene oxide supported Ppy/CdS nanocomposites for the degradation of organic pollutants. *Journal of Photochemistry and Photobiology A: Chemistry*. 2020; **386**:112129

[52] Kovačič Z, Likozar B, Hus M. Photocatalytic CO₂ reduction: A review of ab initio mechanism, kinetics, and multiscale modeling simulations. *ACS Catalysis*. 2020; **10**:14984-15007

[53] Lettmann C, Hildenbrand K, Kisch H, Macyk W, Maier WF. Visible light photodegradation of 4-chlorophenol with a coke-containing titanium dioxide photocatalyst. *Applied Catalysis B: Environmental*. 2001; **32**: 215-227

[54] Anucha CB, Altin I, Bacaksiz E, Stathopoulos VN. Titanium dioxide (TiO₂)-based photocatalyst materials activity enhancement for contaminants of emerging concern (CECs) degradation: In the light of modification strategies. *Chemical Engineering Journal Advances*. 2022; **10**:100262

[55] Weller H. Quantized semiconductor particles: A novel state of matter for materials science. *Advanced Materials*. 1993; **5**(2):88-95

[56] Esteves ACC, Trindade, T. Synthetic studies on II/VI semiconductor quantum dots. *Current Opinion in Solid*

State & Materials Science. 2002;**6**(4): 347-353

[57] Gaya UI. Heterogeneous Photocatalysis Using Inorganic Semiconductor Solids. Drordrecht, New York: Springer; 2014. pp. 1-213

[58] El-Sayed MA. Small is different: Shape-, size-, and composition-dependent properties of some colloidal semiconductor nanocrystals. Accounts of Chemical Research. 2004; **37**:326-333

[59] Mgabi LP, Dladla BS, Malik MA, Garje SS, Akhtar J, Revaprasadu N. Deposition of cobalt and nickel sulfide thin films from thio- and alkylthio-urea complexes as precursors via the aerosol assisted chemical vapour deposition technique. Thin Solid Films. 2014;**564**: 51-57

[60] Gosavi SR, Nikam CP, Shelke AR, Patil AM, Ryu SW, Bhat JS, et al. Chemical synthesis of porous web-structured CdS thin films for photosensor applications. Materials Chemistry and Physics. 2015;**160**: 244-250

[61] Vakalopoulou E, Rath T, Kräuter M, Torvisco A, Fischer RC, Kunert B, et al. Metal sulfide thin films with tunable nanoporosity for photocatalytic applications. ACS Applied Nano Materials. 2022;**5**:1508-1520

[62] Trindade T, Brien PO, Pickett NL. Nanocrystalline semiconductors: Synthesis, properties, and perspectives. Chemistry of Materials. 2001;**13**: 3843-3858

[63] Smith AM, Nie S. Semiconductor nanocrystals: Structure, properties, and band gap engineering. Accounts of Chemical Research. 2010;**43**: 190-200

[64] Brus LE. Electron-electron and electron-hole interactions in small semiconductor crystallites: The size dependence of the lowest excited electronic state. The Journal of Chemical Physics. 1984;**80**:4403-4409

[65] Vogel R, Pohl K, Weller H. Sensitization of highly porous, polycrystalline TiO₂ electrodes by quantum sized CdS. Chemical Physics Letters. 1990;**174**:241-246

[66] Vogel R, Hoyer P, Weller H. Quantum-sized PbS, CdS, Ag₂S, Sb₂S₃, and Bi₂S₃ particles as sensitizers for various nanoporous wide-bandgap semiconductors. The Journal of Physical Chemistry. 1994;**98**:3183-3188

[67] Baker DR, Kamat PV. Photosensitization of TiO₂ nanostructures with CdS quantum dots: Particulate versus tubular support architectures. Advanced Functional Materials. 2009;**19**:805-811

[68] Tang A, Qu S, Li K, Hou Y, Teng F, Cao J, et al. One-pot synthesis and self-assembly of colloidal copper(I) sulfide nanocrystals. Nanotechnology. 2010;**21**: 285602

[69] Kadlag KP, Rao MJ, Nag A. Ligand-free, colloidal, and luminescent metal sulfide nanocrystals. Journal of Physical Chemistry Letters. 2013;**4**: 1676-1681

[70] Smagin VP, Davydov DA, Unzhakova NM, Biryukov AA. Synthesis and spectral properties of colloidal solutions of metal sulfides. Russian Journal of Inorganic Chemistry. 2015;**60**: 1588-1593

[71] Giansante C. Surface chemistry control of colloidal quantum dot band

gap. *Journal of Physical Chemistry C*. 2018;**122**:18110-18116

[72] Zhuang TT, Liu Y, Li Y, Zhao Y, Wu L, Jiang J, et al. Integration of semiconducting sulfides for full-spectrum solar energy absorption and efficient charge separation. *Angewandte Chemie International Edition*. 2016;**55**: 6396-6400

[73] Weng B, Qi MY, Han C, Tang ZR, Xu YJ. Photocorrosion inhibition of semiconductor-based photocatalysts: Basic principle, current development, and future perspective. *ACS Catalysis*. 2019;**9**:4642-4687

[74] Lang D, Xiang Q, Qiu G, Feng X, Liu F. Effects of crystalline phase and morphology on the visible light photocatalytic H₂-production activity of CdS nanocrystals. *Dalton Transactions*. 2014;**43**:7245-7253

[75] Chen J, Wu XJ, Yin L, Li B, Hong X, Fan Z, et al. One-pot synthesis of CdS nanocrystals hybridized with single-layer transition-metal dichalcogenide nanosheets for efficient photocatalytic hydrogen evolution. *Angewandte Chemie International Edition*. 2015;**54**: 1210-1214

[76] Zhang K, Kim W, Ma M, Shi X, Park JH. Tuning the charge transfer route by p-n junction catalysts embedded with CdS nanorods for simultaneous efficient hydrogen and 7oxygen evolution. *Journal of Materials Chemistry A*. 2015;**3**(9): 4803-4810

[77] Huang H, Dai B, Wang W, Lu C, Kou J, Ni Y, et al. Oriented built-in electric field introduced by surface gradient diffusion doping for enhanced photocatalytic H₂ evolution in CdS nanorods. *Nano Letters*. 2017;**17**: 3803-3808

[78] Xie YP, Yu ZB, Liu G, Ma XL, Cheng HM. CdS-mesoporous ZnS core-shell particles for efficient and stable photocatalytic hydrogen evolution under visible light. *Energy & Environmental Science*. 2014;**7**:1895-1901

[79] Bo T, Wang Y, Wang J, Zhao Z, Zhang J, Zheng K, et al. Photocatalytic H₂ evolution on CdS modified with partially crystallized MoS₂ under visible light irradiation. *Chemical Physics Letters*. 2020;**746**:137305

[80] Li P, He T. Common-cation based Z-scheme ZnS@ZnO core-shell nanostructure for efficient solar-fuel production. *Applied Catalysis B: Environmental*. 2018;**238**:518-524

[81] Tian B, Yang B, Li J, Li Z, Zhen W, Wu Y, et al. Water splitting by CdS/Pt/WO₃-CeO_x photocatalysts with assisting of artificial blood perfluorodecalin. *Journal of Catalysis*. 2017;**350**:189-196

[82] Berr MJ, Wagner P, Fischbach S, Vaneski A, Schneider J, Sussha AS, et al. Hole scavenger redox potentials determine quantum efficiency and stability of Pt-decorated CdS nanorods for photocatalytic hydrogen generation. *Applied Physics Letters*. 2012;**100**: 223903

[83] Davis AP, Huang CP. The photocatalytic oxidation of sulfur-containing organic compounds using cadmium sulfide and the effect on CdS photocorrosion. *Water Research*. 1991;**25**:1273-1278

[84] Huang L, Wang X, Yang J, Liu G, Han J, Li C. Dual cocatalysts loaded type I CdS/ZnS core/shell nanocrystals as effective and stable photocatalysts for H₂ evolution. *Journal of Physical Chemistry C*. 2013;**117**:11584-11591

- [85] Yi X, Li H, Wang P, Fan J, Yu H. Boosting antiphotocorrosion and hydrogen-production activity of cadmium sulfide by cobalt lactate complex. *Applied Surface Science*. 2020; **512**:144786
- [86] Wang P, Li H, Sheng Y, Chen F. Inhibited photocorrosion and improved photocatalytic H²-evolution activity of CdS photocatalyst by molybdate ions. *Applied Surface Science*. 2019; **463**:27-33
- [87] Aral Dhas N, Zaban A, Gedanken A. Surface synthesis of zinc sulfide nanoparticles on silica microspheres: Sonochemical preparation, characterization, and optical properties. *Chemistry of Materials*. 1999; **11**(3): 806-813
- [88] Monteiro OC, Esteves ACC, Trindade T. The synthesis of SiO₂@CdS nanocomposites using single-molecule precursors. *Chemistry of Materials*. 2002; **14**(7):2900-2904
- [89] Lv XJ, Fu WF, Chang HX, Zhang H, Cheng JS, Zhang GJ, et al. Hydrogen evolution from water using semiconductor nanoparticle/graphene composite photocatalysts without noble metals. *Journal of Materials Chemistry*. 2012; **22**:1539-1546
- [90] Han L, Wang P, Dong S. Progress in graphene-based photoactive nanocomposites as a promising class of photocatalyst. *Nanoscale*. 2012; **4**: 5814-5825
- [91] Radich JG, Krenselewski AL, Zhu J, Kamat PV. Is graphene a stable platform for photocatalysis? Mineralization of reduced graphene oxide with UV-irradiated TiO₂ nanoparticles. *Chemistry of Materials*. 2014; **26**:4662-4668
- [92] Putri LK, Tan LL, Ong WJ, Chang WS, Chai SP. Graphene oxide: Exploiting its unique properties toward visible-light-driven photocatalysis. *Applied Materials Today*. 2016; **4**:9-16
- [93] Tiwari S, Jhamb N, Kumar S, Ganguli AK. Synthesis of photocorrosion-resistant VS₄-MoS₂-rGO based nanocomposite with efficient photoelectrochemical water-splitting activity. *ChemNanoMat*; 2022; **8**:3
- [94] Wang W, Tao Y, Fan J, Yan Z, Shang H, Phillips DL, et al. Fullerene-Graphene acceptor drives ultrafast carrier dynamics for sustainable CdS photocatalytic hydrogen evolution. *Advanced Functional Materials*. 2022; **32**: 2201357
- [95] Georgakilas V, Perman JA, Tucek J, Zboril R. Broad family of carbon nanoallotropes: Classification, chemistry, and applications of fullerenes, carbon dots, nanotubes, graphene, nanodiamonds, and combined superstructures. *Chemical Reviews*. 2015; **115**:4744-4822
- [96] Hontoria-Lucas C, López-Peinado AJ, López-González J, Rojas-Cervantes ML, Martín-Aranda RM. Study of oxygen-containing groups in a series of graphite oxides: Physical and chemical characterization. *Carbon*. 1995; **33**(11): 1585-1592
- [97] Cai M, Thorpe D, Adamson DH, Schniepp HC. Methods of graphite exfoliation. *Journal of Materials Chemistry*. 2012; **22**(48):24992-25002
- [98] Spyrou K, Rudolf P. An Introduction to Graphene. In: Georgakilas V, editor. *Functionalization of Graphene*. Weinheim, Germany: Wiley VCH; 2014. pp. 1-18
- [99] Zhu Y, Murali S, Cai W, Li X, Suk JW, Potts JR, et al. Graphene and

graphene oxide: Synthesis, properties, and applications. *Advanced Materials*. 2010;**22**:3906-3924

[100] Boukhvalov DW, Katsnelson MI. Chemical functionalization of graphene with defects. *Nano Letters*. 2008;**8**(12): 4374-4379

[101] Ciesielski A, Samorì P. Graphene via sonication assisted liquid-phase exfoliation. *Chemical Society Reviews*. 2014;**43**(1):381-398

[102] Jilani A, Othman MHD, Ansari MO, Hussain SZ, Ismail AF, Khan IU, et al. Graphene and its derivatives: Synthesis, modifications, and applications in wastewater treatment. *Environmental Chemistry Letters*. 2018; **16**:1301-1323

[103] Bourlinos AB, Georgakilas V, Zboril R, Sterioti TA, Stubos AK. Liquid-phase exfoliation of graphite towards solubilized graphenes. *Small*. 2009; **5**(16):1841-1845

[104] Khan U, Porwal H, Óneill A, Nawaz K, May P, Coleman JN. Solvent-exfoliated graphene at extremely high concentration. *Langmuir*. 2011;**27**: 9077-9082

[105] Coleman JN. Liquid exfoliation of defect-free graphene. *Accounts of Chemical Research*. 2013;**46**:14-22

[106] Hernandez Y, Nicolosi V, Lotya M, Blighe FM, Sun Z, De S, et al. High-yield production of graphene by liquid-phase exfoliation of graphite. *Nature Nanotechnology*. 2008;**3**: 563-568

[107] Compton OC, Nguyen ST. Graphene oxide, highly reduced graphene oxide, and graphene: Versatile building blocks for carbon-based materials. *Small*. 2010;**6**:711-723

[108] Wang HX, Wang Q, Zhou KG, Zhang HL. Graphene in light: Design, synthesis and applications of photo-active graphene and graphene-like materials. *Small*. 2013;**8**:1266-1283

[109] Lerf A, Buchsteiner A, Pieper J, Schöttl S, Dekany I, Szabo T, et al. Hydration behavior and dynamics of water molecules in graphite oxide. *Journal of Physics and Chemistry of Solids*. 2006;**67**:1106-1110

[110] Saleh TA. The Role of Carbon Nanotubes in Enhancement of Photocatalysis. In: Suzuki S, editor. *Syntheses and Applications of Carbon Nanotubes and Their Composites*. London: IntechOpen; 2013. pp. 479-494

[111] Liu Z, Tabakman S, Welsher K, Dai H. Carbon nanotubes in biology and medicine: In vitro and in vivo detection, imaging and drug delivery. *Nano Research*. 2009;**2**:85-120

[112] Soulie-Ziakovic C, Nicolay R, PrevotEAU A, Leibler L. Dispersible carbon nanotubes. *Chemistry A European Journal*. 2014;**20**(5):1210-1217

[113] Estrada AC, Mendoza E, Trindade T. Decoration of carbon nanostructures with metal sulfides by sonolysis of single-molecule precursors. *European Journal of Inorganic Chemistry*. 2015;**2014**:3184-3190

[114] Allen MJ, Tun VC, Kaner RB. Honeycomb carbon: A review of graphene. *Chemical Reviews*. 2010;**110**: 132-145

[115] Lopes JL, Fateixa S, Estrada AC, Gouveia JD, Gomes JRB, Trindade T. Surface-enhanced Raman scattering due to a synergistic effect on ZnS and graphene oxide. *Journal of Physical Chemistry C*. 2020;**124**(23):12742-12751

- [116] Hao H, Lang X. Metal sulfide photocatalysis: Visible-Light-induced organic transformations. *ChemCatChem*. 2019;**11**:1378-1393
- [117] Mondal A, Prabhakaran A, Gupta S, Subramanian VR. Boosting photocatalytic activity using reduced graphene oxide (RGO)/semiconductor nanocomposites: Issues and future scope. *ACS Omega*. 2021;**6**:8734-8743
- [118] Hu Y, Zhou C, Wang H, Chen M, Zeng G, Liu Z, et al. Recent advance of graphene/semiconductor composite nanocatalysts: Synthesis, mechanism, applications and perspectives. *Chemical Engineering Journal*. 2021;**414**:128795
- [119] Sun Y, Li G, Xu J, Lei B, Feng H, Sun Z. Impacts of graphene sheets on photoelectric and photocatalytic activities of SnS₂ nanoparticles. *Materials Chemistry and Physics*. 2019;**229**:92-97
- [120] Chen FJ, Cao YL, Jia DZ. A room-temperature solid-state route for the synthesis of graphene oxide-metal sulfide composites with excellent photocatalytic activity. *CrystEngComm*. 2013;**15**(23):4747-4754
- [121] Shi J, Zhou X, Liu Y, Su Q, Zhang J, Du G. Sonochemical synthesis of CuS/reduced graphene oxide nanocomposites with enhanced absorption and photocatalytic performance. *Materials Letters*. 2014;**126**:220-223
- [122] Zou L, Wang X, Xu X, Wang H. Reduced graphene oxide wrapped CdS composites with enhanced photocatalytic performance and high stability. *Ceramics International*. 2016;**42**:372-378
- [123] Azimi HR, Ghoranneviss M, Elahi SM, Mahmoudian MR, Jamali-Sheini F, Yousefi R. Excellent photocatalytic performance under visible-light irradiation of ZnS/rGO nanocomposites synthesized by a green method. *Frontiers of Materials Science*. 2016;**10**(4):385-393
- [124] Liu F, Shao X, Wang J, Yang S, Li H, Meng X, et al. Solvothermal synthesis of graphene-CdS nanocomposites for highly efficient visible-light photocatalyst. *Journal of Alloys and Compounds*. 2013;**551**:327-332
- [125] Mo Z, Liu P, Guo R, Deng Z, Zhao Y, Sun Y. Graphene sheets/Ag₂S nanocomposites: Synthesis and their application in supercapacitor materials. *Materials Letters*. 2012;**68**:416-418
- [126] Kaur M, Umar A, Mehta SK, Kansal SK. Reduced graphene oxide-CdS heterostructure: An efficient fluorescent probe for the sensing of Ag(I) and sunset yellow and a visible-light responsive photocatalyst for the degradation of levofloxacin drug in aqueous phase. *Applied Catalysis B: Environmental*. 2019;**245**:143-158
- [127] Sagadevan S, Chowdhury ZZ, Bin JMR, Rafique RF, Aziz FA. One pot synthesis of hybrid ZnS-Graphene nanocomposite with enhanced photocatalytic activities using hydrothermal approach. *Journal of Materials Science: Materials in Electronics*. [Internet. 2018;**29**(11):9099-9107. Available from: DOI: 10.1007/s10854-018-8937-z
- [128] Wei XN, Ou CL, Guan XX, Peng ZK, Zheng XC. Facile assembly of CdS-reduced graphene oxide heterojunction with enhanced elimination performance for organic pollutants in wastewater. *Applied Surface Science*. 2019;**469**:666-673

- [129] Yu L, Ruan H, Zheng Y, Li D. A facile solvothermal method to produce ZnS quantum dots-decorated graphene nanosheets with superior photoactivity. *Nanotechnology*. 2013;**24**: 375601
- [130] Zhang Y, Zhang N, Tang ZR, Xu YJ. Graphene transforms wide band gap ZnS to a visible light photocatalyst. the new role of graphene as a macromolecular photosensitizer. *ACS Nano*. 2012;**6**(11): 9777-9789
- [131] Lopes J, Estrada A, Fateixa S, Ferro M, Trindade T. A general route for growing metal sulfides onto graphene oxide and exfoliated graphite oxide. *Nanomaterials*. 2017;**7**:245
- [132] Bai S, Shen X, Zhu G, Zhou H, Xu H, Fu G, et al. Optical properties and a simple and general route for the rapid syntheses of reduced graphene oxide-metal sulfide nanocomposites. *European Journal of Inorganic Chemistry*. 2013;**2**: 256-262
- [133] Hu H, Wang X, Liu F, Wang J, Xu C. Rapid microwave-assisted synthesis of graphene nanosheets-zinc sulfide nanocomposites: Optical and photocatalytic properties. *Synthetic Metals*. 2011;**161**:404-410
- [134] Liu X, Pan L, Lv T, Zhu G, Sun Z, Sun C. Microwave-assisted synthesis of CdS-reduced graphene oxide composites for photocatalytic reduction of Cr(VI). *Chemical Communications*. 2011;**47**: 11984-11986
- [135] Thangavel S, Krishnamoorthy K, Kim SJ, Venugopal G. Designing ZnS decorated reduced graphene-oxide nanohybrid via microwave route and their application in photocatalysis. *Journal of Alloys and Compounds*. 2016; **683**:456-462
- [136] Chen F, Cao Y, Jia D, Liu A. Solid-state synthesis of ZnS/graphene nanocomposites with enhanced photocatalytic activity. *Dyes and Pigments*. 2015;**120**:8-14
- [137] Chen Y, Tian G, Mao G, Li R, Xiao Y, Han T. Facile synthesis of well-dispersed Bi₂S₃ nanoparticles on reduced graphene oxide and enhanced photocatalytic activity. *Applied Surface Science*. 2016;**378**:231-238
- [138] Hull S, Keen DA, Sivia DS, Madden PA, Wilson M. The high-temperature superionic behaviour of Ag₂S. *Journal of Physics Condensed Matter*. 2002;**14**:L9-L17
- [139] Sharma S, Dutta V, Raizada P, Hosseini-Bandegharai A, Singh P, Nguyen VH. Tailoring cadmium sulfide-based photocatalytic nanomaterials for water decontamination: A review. *Environmental Chemistry Letters*. 2021; **19**:271-306
- [140] Zhang N, Yang MQ, Tang ZR, Xu YJ. CdS-graphene nanocomposites as visible light photocatalyst for redox reactions in water: A green route for selective transformation and environmental remediation. *Journal of Catalysis*. 2013;**303**:60-69
- [141] Wang L, Wen M, Wang W, Momuinou N, Wang Z, Li S. Photocatalytic degradation of organic pollutants using rGO supported TiO₂-CdS composite under visible light irradiation. *Journal of Alloys and Compounds*. 2016;**683**:318-328
- [142] Tian Z, Yu N, Cheng Y, Wang Z, Chen Z, Zhang L. Hydrothermal synthesis of graphene/TiO₂/CdS nanocomposites as efficient visible-light-driven photocatalysts. *Materials Letters*. 2017;**194**:172-175

- [143] Liu T, Liu B, Yang L, Ma X, Li H, Yin S, et al. RGO/Ag₂S/TiO₂ ternary heterojunctions with highly enhanced UV-NIR photocatalytic activity and stability. *Applied Catalysis B: Environmental*. 2017;**204**:593-601
- [144] Wang J, Zhang X, Wu J, Chen H, Sun S, Bao J, et al. Preparation of Bi₂S₃/carbon quantum dot hybrid materials with enhanced photocatalytic properties under ultraviolet-, visible- and near infrared-irradiation. *Nanoscale*. 2017;**9**: 15873-15882
- [145] Khalid A, Akhtar N, He K, Liu B, Ahmad M, Ambreen J, et al. Bismuth sulfide photocatalysis water treatment under visible irradiation. *Research on Chemical Intermediates*. 2021;**47**: 3395-3409
- [146] Hu W, Zhao L, Zhang Y, Zhang X, Dong L, Wang S. Preparation and photocatalytic activity of graphene-modified Ag₂S composite. *Journal of Experimental Nanoscience*. 2016;**11**: 433-443
- [147] Cao Q, Che R, Chen N. Scalable synthesis of Cu₂S double-superlattice nanoparticle systems with enhanced UV/visible-light-driven photocatalytic activity. *Applied Catalysis B: Environmental*. 2015;**162**:187-195
- [148] Srinivas B, Kumar BG, Muralidharan K. Stabilizer free copper sulphide nanostructures for rapid photocatalytic decomposition of rhodamine B. *Journal of Molecular Catalysis A: Chemical*. 2015;**410**:8-18
- [149] Ayodhya D, Venkatesham M, Santoshi kumari A, Reddy GB, Ramakrishna D, Veerabhadram G. Photocatalytic degradation of dye pollutants under solar, visible and UV lights using green synthesised CuS nanoparticles. *Journal of Experimental Nanoscience*. 2016;**11**(6):418-432
- [150] Li S, Zhang Z, Yan L, Jiang S, Zhu N, Li J, et al. Fast synthesis of CuS and Cu₉S₅ microcrystal using subcritical and supercritical methanol and their application in photocatalytic degradation of dye in water. *Journal of Supercritical Fluids*. 2017;**123**:11-17
- [151] Wu H, Li Y, Li Q. Facile synthesis of CuS nanostructured flowers and their visible light photocatalytic properties. *Applied Physics A: Materials Science & Processing*. 2017;**123**:196
- [152] Estrada AC, Silva FM, Soares SF, Coutinho JAP, Trindade T. An ionic liquid route to prepare copper sulphide nanocrystals aiming at photocatalytic applications. *RSC Advances*. 2016;**6**(41): 34521-34528
- [153] Zhang Y, Tian J, Li H, Wang L, Qin X, Asiri AM, et al. Biomolecule-assisted, environmentally friendly, one-pot synthesis of CuS/reduced graphene oxide nanocomposites with enhanced photocatalytic performance. *Langmuir*. 2012;**28**:12893-12900
- [154] Hu XS, Shen Y, Zhang YT, Nie JJ. Preparation of flower-like CuS/reduced graphene oxide(RGO) photocatalysts for enhanced photocatalytic activity. *Journal of Physics and Chemistry of Solids*. 2017;**103**:201-208
- [155] Saranya M, Ramachandran R, Kollu P, Jeong SK, Grace AN. A template-free facile approach for the synthesis of CuS-rGO nanocomposites towards enhanced photocatalytic reduction of organic contaminants and textile effluents. *RSC Advances*. 2015;**5**: 15831-15840
- [156] Siong VLE, Lee KM, Juan JC, Lai CW, Tai XH, Khe CS. Removal of

methylene blue dye by solvothermally reduced graphene oxide: A metal-free adsorption and photodegradation method. *RSC Advances*. 2019;**9**: 37686-37695

[157] El-Hout SI, El-Sheikh SM, Gaber A, Shawky A, Ahmed AI. Highly efficient sunlight-driven photocatalytic degradation of malachite green dye over reduced graphene oxide-supported CuS nanoparticles. *Journal of Alloys and Compounds*. 2020;**849**:156573

[158] Matos R, Nunes MS, Kuźniarska-Biernacka I, Rocha M, Guedes A, Estrada AC, et al. Graphene@metal sulfide/oxide nanocomposites as novel photo-fenton-like catalysts for 4-nitrophenol degradation. *European Journal of Inorganic Chemistry*. 2021;**47**: 4915-4928

[159] Wang Y, Zhang L, Jiu H, Li N, Sun Y. Depositing of CuS nanocrystals upon the graphene scaffold and their photocatalytic activities. *Applied Surface Science*. 2014;**303**:54-60

[160] Ming F, Hong J, Xu X, Wang Z. Dandelion-like ZnS/carbon quantum dots hybrid materials with enhanced photocatalytic activity toward organic pollutants. *RSC Advances*. 2016;**6**: 31551-31558

[161] Chakraborty K, Chakraborty S, Das P, Ghosh S, Pal T. UV-assisted synthesis of reduced graphene oxide zinc sulfide composite with enhanced photocatalytic activity. *Materials Science & Engineering B*. 2016;**204**:8-14